

Effect of mesh size on the performance of Teflon bonded oxygen-evolving electrodes

J. C. BOTEJUE NADESAN, A. C. C. TSEUNG

Chemical Energy Research Centre, Department of Chemistry, The City University, Northampton Square, London EC1V 0HB, UK

Received 16 October 1984; revised 28 November 1984

Teflon bonded and porous NiCo_2O_4 electrodes were prepared on nickel current collectors of different mesh sizes. It was shown that the oxygen evolution performance of the Teflon bonded electrodes is affected more significantly by the size of the nickel mesh than that of the porous electrodes. A simple theoretical calculation of the ohmic losses showed that for large mesh openings (20 mesh), the Teflon bonded catalyst in the centre of the opening cannot be efficiently utilized because of high ohmic resistances. Provided smaller hole size meshes (eg. 100 mesh) are used, Teflon bonded electrodes perform significantly better than porous electrodes.

1. Introduction

Teflon bonded electrodes have been used in fuel cells and metal air batteries for a long time [1–3]. Basically, the electrode consists of two continuous porous phases: the hydrophilic catalytic phase and the hydrophobic Teflon phase, supported on nickel mesh. In use, the catalytic phase is flooded with electrolyte while the hydrophobic phase provides easy channels for gas diffusion. Hence, the available catalyst surface can be more efficiently utilized and is therefore more preferable to porous electrode structures [4–8].

Teflon bonded electrodes have been scaled up to 300 cm^2 in size by Dams *et al.* [9] and the performance compared favourably with laboratory size electrodes. However, recent work by Haenen *et al.* [10] has suggested that there is basically no difference between the performance of a Teflon bonded and a porous electrode. Therefore, it is necessary to investigate the possible reasons for the different results obtained by the various laboratories. In this paper the effect of nickel mesh sizes on the oxygen evolution performance of both types of electrodes are evaluated.

2. Experimental details

2.1. NiCo_2O_4 catalysts

The catalyst, NiCo_2O_4 , for the Teflon bonded electrodes was synthesized by a coprecipitation technique. First 40 g of Analar $\text{CoCl}_2 \cdot 6\text{H}_2\text{O}$ and 20 g of Analar $\text{NiCl}_2 \cdot 6\text{H}_2\text{O}$ were dissolved in 300 cm^3 of distilled water. The precipitate was made by adding the mixed ionic solution to 250 cm^3 of 3 mol dm^{-3} KOH at ambient temperature. The precipitate was filtered, washed free of alkali, and then dried at 100°C for 1 h in air. The spinel structure was formed by sintering the dried product at 400°C for 5 h in air. For the thermally decomposed electrodes the catalyst was synthesized by decomposing a dilute solution of cobalt and nickel nitrate. In order to prepare 100 cm^3 of solution, 20 g of Analar $\text{Co}(\text{NO}_3)_2 \cdot 6\text{H}_2\text{O}$ and 10 g of Analar $\text{Ni}(\text{NO}_3)_2 \cdot 6\text{H}_2\text{O}$ were used.

The spinel structure of the catalyst prepared by both techniques was confirmed by X-ray diffraction analysis. The specific surface area of the precipitated catalyst was $80\text{ m}^2\text{ g}^{-1}$ and that of the thermally decomposed catalyst $20\text{ m}^2\text{ g}^{-1}$.

Table 1. Physical dimensions of the various nickel mesh

Mesh size	Total Ni area (cm^2)	Distance between two adjacent Ni wires (cm)	Area of one hole (cm^2)	Thickness of the wire (cm)
100	7.5	2.56×10^{-3}	6.55×10^{-6}	2.25×10^{-2}
60	6.96	7.30×10^{-3}	53.3×10^{-6}	3.65×10^{-2}
40	6.3	1.66×10^{-2}	2.70×10^{-4}	4.70×10^{-2}
20	5.4	3.67×10^{-2}	13.5×10^{-4}	6.70×10^{-2}

2.2. Nickel mesh

Nickel meshes of size 100, 60, 40 and 20 were used in the study. The meshes were supplied by the International Nickel Company (UK) Ltd. The current collectors in all the experiments consisted of a 1 cm^2 piece of nickel mesh spot-welded on to a nickel wire. The physical dimensions of the different mesh sizes are tabulated in Table 1, the openings of all the mesh being square shaped.

2.3. Electrode fabrication

The Teflon polymer used for the preparation of Teflon bonded electrodes was an aqueous solution of Teflon 120 FEP (fluorinated ethylene propylene) fluorocarbon resin. The catalyst powder and FEP, in the ratio 3:1, were mixed in methanol and the resulting slurry painted on to the nickel screens. The electrodes were then cured by heating at 300°C for 1 h.

Thermally decomposed electrodes were prepared by dipping the nickel mesh current collectors in the dilute solution of Analar $\text{Ni}(\text{NO}_3)_2 \cdot 6\text{H}_2\text{O}$ and $\text{Co}(\text{NO}_3)_2 \cdot 6\text{H}_2\text{O}$ and drying at 300°C for 5 min. This procedure was repeated until the required loadings were obtained. The electrodes were then sintered at 400°C for 5 h.

2.4. Electrochemical evaluation

The oxygen evolution performance of the electrodes was tested at 25°C in a thermostated, three compartment glass cell. The electrodes were mounted in the submerged mode in 5 mol dm^{-3} KOH electrolyte, prepared by dissolving Analar KOH pellets in doubly distilled

deionized water. A piece of platinum mesh was used as the secondary electrode. The potentials were measured against the reversible hydrogen electrode (RHE) and all the electrodes were preanodized so as to stabilize surface conditions. The preanodizing conditions for the electrodes fabricated with catalyst-FEP were 1 A cm^{-2} at 50°C in 5 mol dm^{-3} KOH for 18 h. The plain nickel electrodes were preanodized at 1 A cm^{-2} for 15 min at 25°C in 5 mol dm^{-3} KOH. A long period of preanodization, as for the catalyst-FEP coated electrodes, was not employed for these electrodes as nickel oxides are formed and this would prevent the observation of the true performance in relation to mesh size. A Chemical Electronics potentiostat (H. B. Thompson, model 251) was used in the galvanostatic mode to obtain the steady state $i-V$ measurements, and the interrupter technique [11] was used to measure the ohmic drop between the Luggin capillary and the working electrode.

3. Results and discussion

3.1. Oxygen evolution performance of the various electrodes

The oxygen evolution performance characteristics of the different nickel meshes are given in Fig. 1. It follows from the results that the oxygen evolution performance increases with the surface area of the nickel wires. The relationship is not linear since the simple calculation in Table 1 does not take into account possible variations in surface roughness of the nickel wires in the different mesh.

Figs 2 and 3 show the variation of oxygen evolution potential with mesh size on FEP bonded electrodes having catalyst loadings of

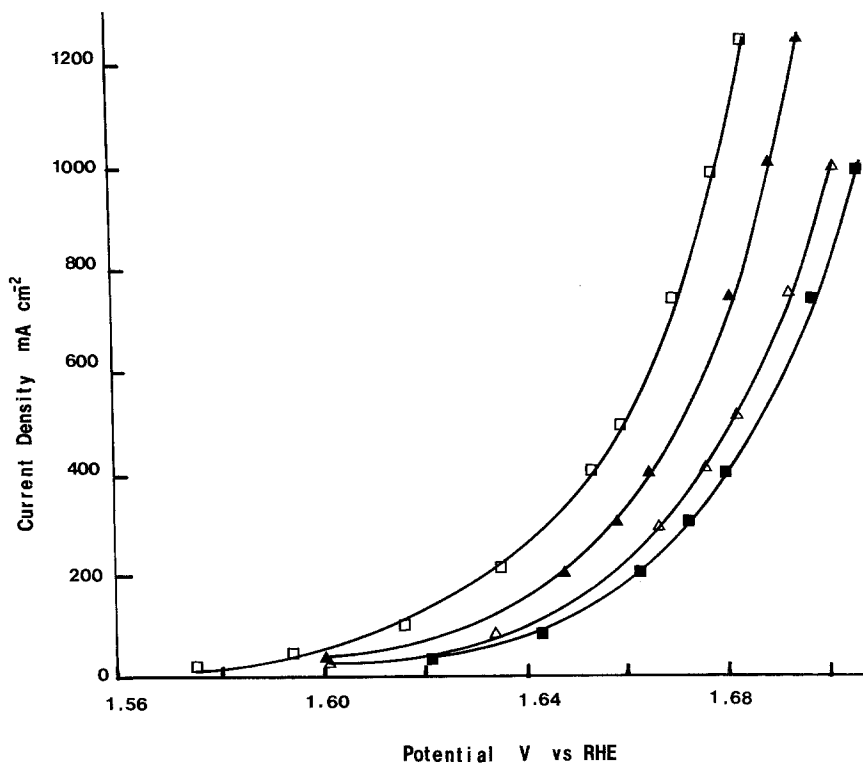


Fig. 1. Current-potential characteristics for the evolution of oxygen on plain nickel mesh current collectors, in 5 mol dm^{-3} KOH at 25°C . (□) 100 mesh; (▲) 60 mesh; (△) 40 mesh; (■) 20 mesh.

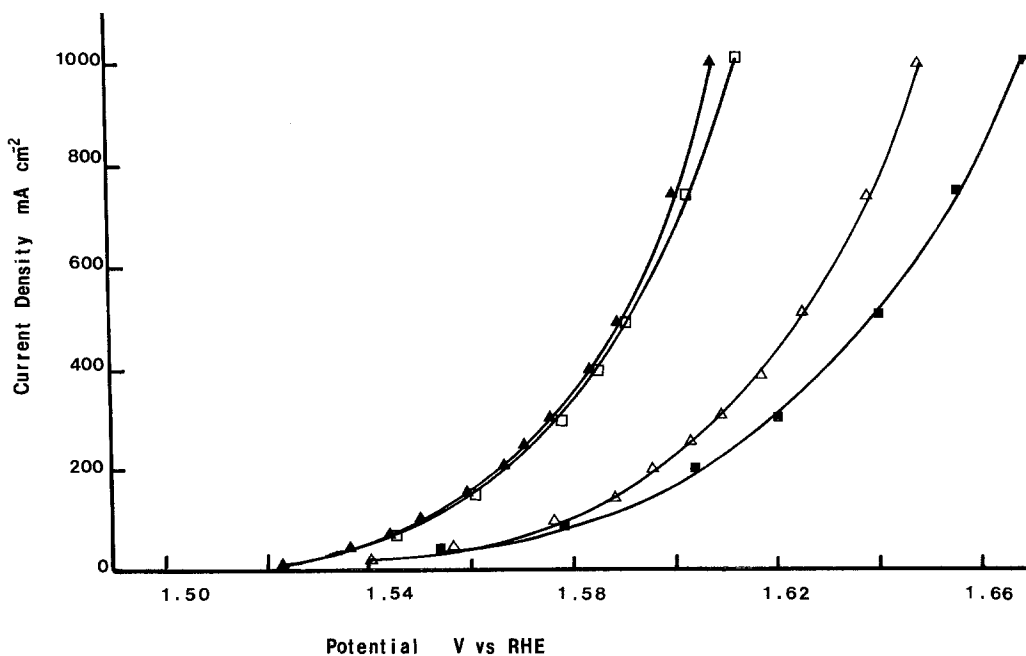


Fig. 2. Current-potential characteristics for the evolution of oxygen on FEP bonded NiCo_2O_4 electrodes of low catalyst loading in 5 mol dm^{-3} KOH at 25°C . (□) 100 mesh, catalyst loading 12.8 mg cm^{-2} ; (▲) 60 mesh, catalyst loading 10.8 mg cm^{-2} ; (△) 40 mesh, catalyst loading 9.37 mg cm^{-2} ; (■) 20 mesh, catalyst loading 12.5 mg cm^{-2} .

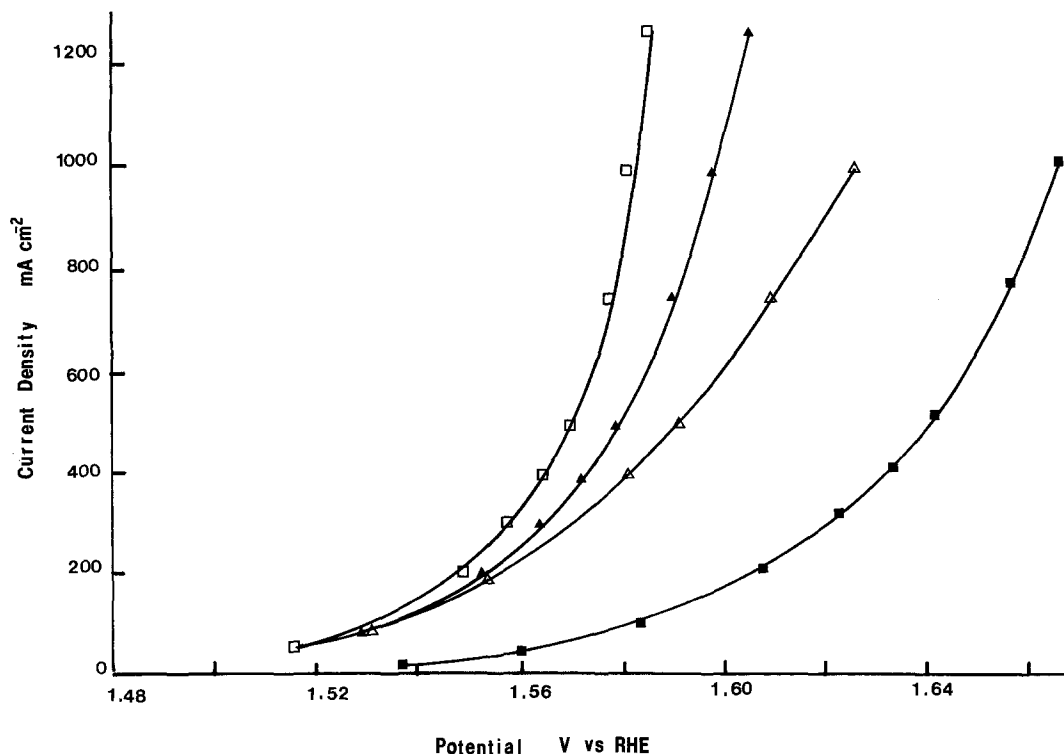


Fig. 3. Current-potential characteristics for the evolution of oxygen on FEP bonded NiCo_2O_4 electrodes of high catalyst loading in $5\text{mol dm}^{-3}\text{KOH}$ at 25°C . (\square) 100 mesh, catalyst loading 21.52 mg cm^{-2} ; (\blacktriangle) 60 mesh, catalyst loading 22.2 mg cm^{-2} ; (\triangle) 40 mesh, catalyst loading 25.57 mg cm^{-2} ; (\blacksquare) 20 mesh, catalyst loading 24.26 mg cm^{-2} .

approximately 10 and $23 \pm 2\text{ mg cm}^{-2}$. Figs 4 and 5 are of the corresponding thermally decomposed electrodes. In the case of coated electrodes at lower loadings ($10 \pm 2\text{ mg cm}^{-2}$) the performance of both classes of electrodes increases with mesh size, and the performance of FEP bonded electrodes is better than that of the thermally decomposed electrodes in all cases. As the loading is increased ($23 \pm 2\text{ mg cm}^{-2}$) there is a significant increase in performance of the FEP bonded electrodes having mesh sizes 100, 60 and 40. The performance of 20 mesh is almost the same. Table 2 compares the oxygen evolution performance of the electrodes. Unlike the FEP bonded electrodes the performance of the 100 and 60 mesh thermally decomposed electrodes decreases with increase of catalyst loading from ~ 10 to $\sim 23\text{ mg cm}^{-2}$. On the other hand the performance of the 40 mesh is better at high loading and that of the 20 mesh is similar at both loadings. This decrease and increase of performance of the thermally decomposed electrodes is related to the covering of the mesh openings. In

Table 2. Oxygen evolution performance of the various electrodes

Mesh	Performance (mA cm^{-2})		
	Plain	FEP [†]	Thermally decomposed [‡]
<i>Plain Ni mesh*</i>			
100		1060	
60		745	
40		450	
20		360	
<i>Low loading ($10 \pm 2\text{ mg}$)</i>			
100		1120	1000
60		1260	880
40		420	390
20		290	180
<i>High loading ($23 \pm 2\text{ mg}$)</i>			
100		2000	340
60		1860	590
40		865	770
20		290	140

*Performance at 1.68 V vs RHE.

[†]Performance at 1.62 V vs RHE.

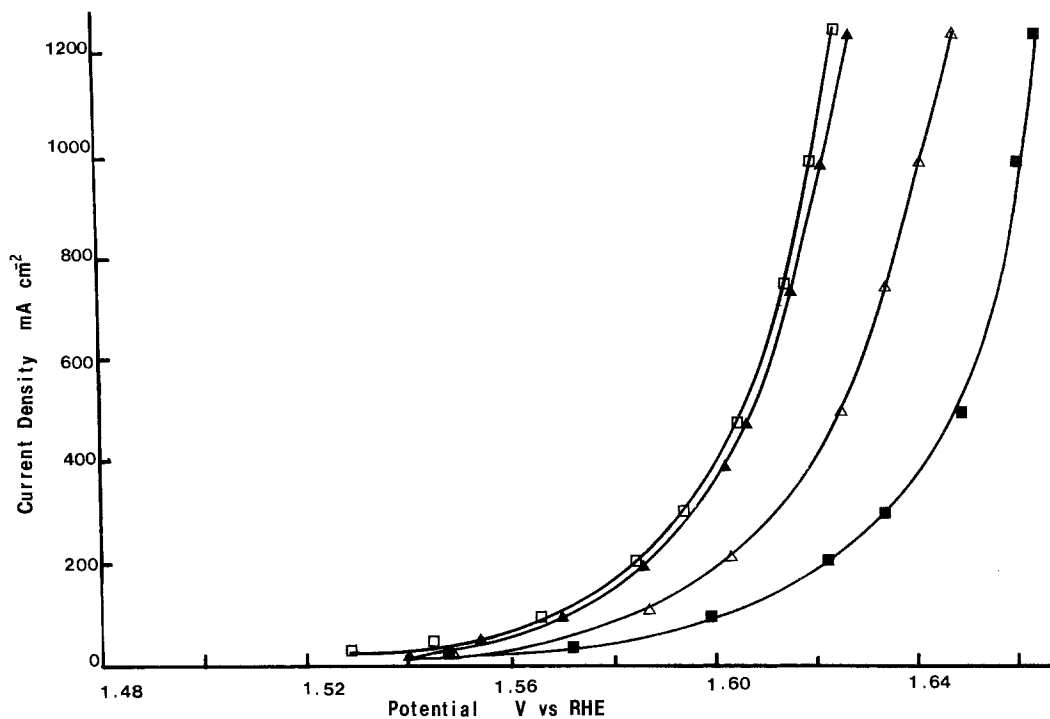


Fig. 4. Current-potential characteristics for the evolution of oxygen on thermally decomposed NiCo_2O_4 electrodes of low catalyst loading, in 5 mol dm^{-3} KOH at 25°C . (\square) 100 mesh, catalyst loading 11.7 mg cm^{-2} ; (\blacktriangle) 60 mesh, catalyst loading 10.27 mg cm^{-2} ; (\triangle) 40 mesh, catalyst loading 8.57 mg cm^{-2} ; (\blacksquare) 20 mesh, catalyst loading 10.7 mg cm^{-2} .

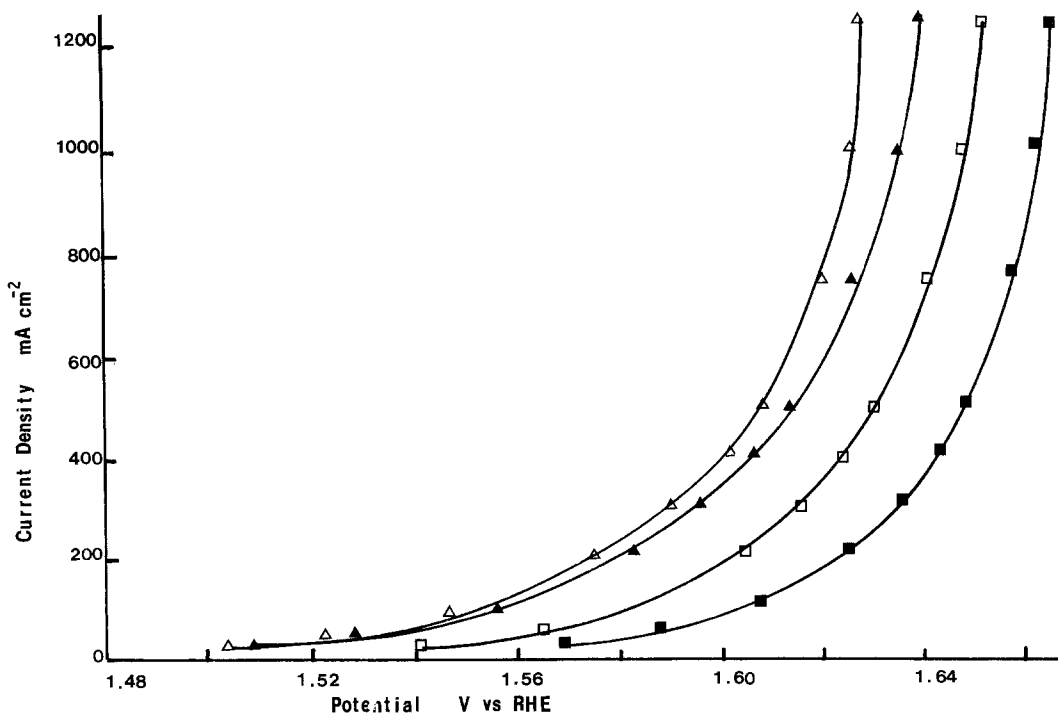


Fig. 5. Current-potential characteristics for the evolution of oxygen on thermally decomposed electrodes of high catalyst loading in 5 mol dm^{-3} KOH at 25°C . (\square) 100 mesh, catalyst loading 23.3 mg cm^{-2} ; (\blacktriangle) 60 mesh, catalyst loading 23.7 mg cm^{-2} ; (\triangle) 40 mesh, catalyst loading 22.9 mg cm^{-2} ; (\blacksquare) 20 mesh, catalyst loading 24.8 mg cm^{-2} .

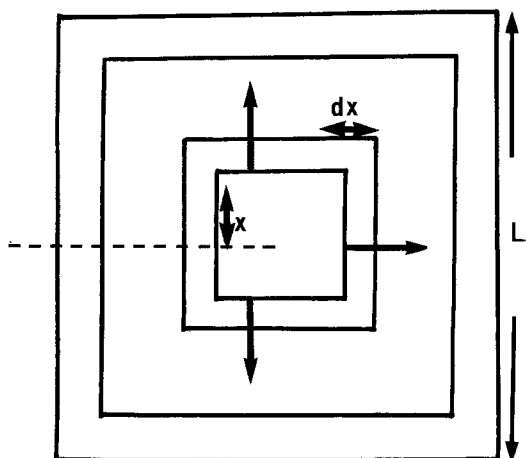


Fig. 6. Schematic diagram showing the current distribution in a single square element of the current collector mesh.

the 40 mesh and 20 mesh thermally decomposed electrodes even at a loading of 23 mg cm^{-2} all of the openings are not completely covered. Hence a greater proportion of the catalyst surface is available for the reaction. On the 100 and 60 mesh at a loading of $\sim 23 \text{ mg cm}^{-2}$ all of the mesh openings are covered by catalyst and only the outer surface can be utilized.

3.2. Calculated ohmic losses as a function of nickel mesh size

The marked effect of mesh sizes on the oxygen evolution performance suggests that the ohmic losses could be different. Fig. 6 shows a simple schematic model for current collection in a single square opening of the nickel mesh.

The current collection efficiency from four sides of the square shaped mesh hole is calculated as follows. Consider a square element of width dx and side $2x$, whose centre is also the centre of the hole; assume that the current generated within each side of this element travels towards the adjacent current collector. Let

hole side = $L(\text{cm})$

current = $I(\text{A})$

current density = $i(\text{A cm}^{-2})$

specific resistivity = $\rho(\text{ohm cm})$

thickness = $t(\text{cm})$

Current generated in central square, $I = 4x^2i$ (1)

Resistance of square element, $R = \rho dx/8xt$ (2)

IR drop across the element,

$$\begin{aligned} \Delta E_{\text{IR}} &= 4x^2 i \rho dx/8xt & (3) \\ &= i \rho x dx/2t \end{aligned}$$

The IR drop in the entire hole (assuming uniform current generated in all parts of the catalyst in each hole) is given by

$$\begin{aligned} \Delta E'_{\text{IR}} &= \frac{i \rho}{2t} \int_0^{L/2} x dx & (4) \\ &= \frac{i \rho L^2}{16t} & (5) \end{aligned}$$

The calculated IR values using the above formula and the measured values of the other parameters indicate very clearly the desirability of using nickel mesh with the smallest holes (Table 3).

It is evident from the calculation that in the case of FEP bonded electrodes supported on

Table 3. Calculated iR values for the two types of electrodes

Mesh	FEP bonded		Thermally decomposed	
	$t (\text{cm} \times 10^{-3})$	IR (mV)	$t (\text{cm} \times 10^{-3})$	IR (mV)
<i>Low loading ($10 \pm 2 \text{ mg cm}^{-2}$)</i>				
100	2.5	4.09	3.5	0.29
60	4.0	20.82	4.5	1.85
40	5.0	85.39	5.5	7.78
20	5.0	420.22	5.0	42.00
<i>High loading ($23 \pm 2 \text{ mg cm}^{-2}$)</i>				
100	9.5	1.07	6.5	0.16
60	5.5	15.14	5.5	1.51
40	5.0	85.39	5.5	7.78
20	5.0	420.20	5.0	42.00

20 mesh nickel screens the calculated IR loss is high. However, the measured IR value for all the electrodes is only in the region of 100 mV at 1000 mA cm^{-2} . This suggests that in such a case only the catalyst nearest to the nickel wires in the 20 mesh screen can be utilized. Hence, the experimentally determined IR drop only measures the ohmic losses from the sites of electrochemical reaction to the nickel wires. In the case of large hole sizes, catalyst in the centre of the hole is not utilized because of the high resistance drop and only the catalyst nearest to the wires can function. This effect is particularly important in the case of Teflon bonded electrodes, because of the higher resistivity of the catalyst-Teflon layer.

4. Conclusions

The above results clearly show the importance of choosing the appropriate mesh size for Teflon bonded electrodes. Provided this is carried out, Teflon bonded electrodes give significantly better performance than the corresponding porous electrodes in all cases.

Acknowledgement

This work was supported by the European Economic Commission.

References

- [1] A. D. S. Tantram and A. C. C. Tseung, *Nature* **221** (1969) 167.
- [2] O. J. Aldhart, 'Proceedings Nineteenth Annual Power Source Conference', PSC Publications Committee, New York (1965) p. 1.
- [3] J. A. Shropshire, R. H. Akrent and H. H. Horowitz, 'Hydrocarbon Fuel Cell Technology' (edited by B. S. Baker) Academic Press, New York (1965) p. 539.
- [4] B. S. Hobbs, P. R. Vassie and A. C. C. Tseung, 'Electrochemical Energy Symposium', Vol. 1 (edited by D. J. Thornton) Institute of Chemical Engineers, London (1971) p. 123.
- [5] P. R. Vassie and A. C. C. Tseung, *Electrochim. Acta* **20** (1975) 759.
- [6] *Idem*, *ibid.* **20** (1975) 763.
- [7] A. C. C. Tseung and P. R. Vassie, *ibid.* **21** (1976) 315.
- [8] A. C. C. Tseung, S. Jasem and M. N. Mahmood, '2nd World Hydrogen Energy Conference', Zurich (edited by T. Z. Veziroglu and A. Seifritz) Pergamon Press, Oxford (1978) Vol. 1, p. 78.
- [9] R. A. J. Dams, R. D. Giles and T. P. Smith, '3rd International Seminar on Hydrogen as an Energy Carrier', Lyon, France (1983) p. 27.
- [10] J. G. D. Haenen, W. Visscher and E. Barendrecht, 'International Society of Electrochemistry, 34th Meeting', Extended Abstracts, Erlangen, Germany (1983) 0303.
- [11] K. R. Williams, 'An Introduction to Fuel Cells', Elsevier, Amsterdam (1966) p. 58.